P-ISSN 2586-9000
E-ISSN 2586-9027
Homepage : https://tci-thaijo.org/index.php/SciTechAsia
Science & Technology Asia
Vol. 28 No.3 July – September 2023
Page: [158-177]
Original research article

Strength, Durability and Bond Characteristics of Hybrid Glass Powder Concrete for Applying as an Overlay

Deepa Paul, Bindhu K. R.*

Department of Civil Engineering, APJ Abdul Kalam Technological University, College of Engineering Trivandrum, Kerala 695016, India

Received 22 May 2023; Received in revised form 20 July 2023
Accepted 23 August 2023; Available online xx Month 201x

ABSTRACT

The potential utilization of fine glass powder (GP) as an eco-cementing material in concrete was experimentally investigated based on the strength, durability, and interface bond characteristics. The current research utilized hybrid GP, combining two micron-sized GPs with different particle sizes in equal proportions, to produce well-graded mixes of M30, M40, and M50. Strength and performance characteristics were experimentally investigated to arrive at a better partial replacement level of cement with hybrid GP. The shear strength of hybrid GP concrete cubes with substrates and repair material of different concrete mixes was also examined. Interface bond strength was evaluated by conducting the slant shear test on concrete prisms with the normal concrete as a substrate and hybrid GP concrete as an overlay. Analyses of the hardened properties revealed that 30% hybrid GP substitution produced the highest compressive strength. The GP concrete mixes exhibited improved performance in the durability indicators like sorptivity, chloride permeation, and moisture movement, but show a marginal increase in drying shrinkage. Tests on the application of hybrid GP concrete as an overlay concrete with conventional concrete as a substrate show a considerable improvement in the interface shear bond characteristics. The studies confirm the recyclability of waste GP as a partial substitute for cement in repair works.

Keywords: Durability characteristics; Glass powder; Glass recycling; Mechanical properties; Supplementary cementing material

1. Introduction

Feasibility of glass powder (GP) as a partial cement replacement material in mortar and concrete was revealed by several authors during the past decade by evaluating its mechanical and durability properties [1-12]. Recent works on the performance of GP concrete focused on the exposure of GP concrete to heat curing [13], resistance of GP concrete to elevated temperatures [14],

*Corresponding author: bindhukr@cet.ac.in
doi: 10.14456/scitechasia.2023.53

dissolution of calcium and sodium ions from GP by the new mixing method [15, 16], behavior of foam concrete with GP [17], hygrothermal properties of concrete containing GP [18], influence of GP in both ultra-high-performance concrete [19] and self-compacting concrete mixes [20], and the combined effects of GP with other supplementary cementitious materials (SCM) like silica fume [21], fly ash [22], ground granulated blast-furnace slag (GGBS) [23], waste granite powder [24], waste E-plastic [25] etc., engrossed the researchers to explore furthermore about the GP composite concrete. Critical review of waste GP as a cementing material by Jiang et al. discussed the effectiveness of GP in cement-based materials, cement-less composites, in sintering products and in heat storage material [26]. The interface bond strength and slant shear failure mode are significant factors that need to be explored before its application in the concrete sector.

Utilisation of waste glass as a building material is studied in the present investigation due to the commendable properties which were reported in the past research. The hydration of cement leads to the formation of calcium silicate hydrate (CSH) crystals and portlandite ($Ca(OH)_2$). Among the hydration products, CSH which imparts strength to the concrete is highly preferable. One of the facts is that the durability of concrete is adversely affected due to crack formation caused by the leaching of calcium [27, 28], while another fact is that the reaction of calcium with sulphates leads to the formation of $CaSO_4$ which in excess is detrimental to concrete [29]. Hence, to overcome the limitations of ordinary Portland cement, silica- rich blending materials which contribute to the generation of CSH crystals are greatly advisable for producing a durable high strength concrete. Dense microstructure of the cement paste containing GP with high pozzolanic activity was observed due to the formation of CSH structure with a low calcium/ silicon ratio [30]. Therefore, non-degradable fine GP, rich in silica, having different particle sizes is considered as a partial substitute for cement in the current study to enhance the strength and durability characteristics.

In order to strengthen the existing concrete or in repair work, new concrete must be placed over the prepared surface of old concrete. Hence determination of adhesion of the repair materials to the existing concrete is of utmost importance in ensuring good bond strength of repaired structures. Since the bond plane forms the weakest link of the repaired concrete structure, parameters like strength of the interface bond, interface angle and composition of both the substrate and overlay of the repaired concrete structures greatly influence its durability. Previous studies of the interface bond characteristics between light- weight aggregate concrete and normal density concrete [31], self-compacting concrete and normal concrete [32], fly ash based alkali activated concrete and Portland cement concrete [33], ultra- high reactive powder and fiber reinforced concrete [34], epoxy resin concrete and normal strength concrete [35], engineered cementitious composites and ordinary concrete substrate [36] demonstrate that the bond strength depends on the composition and the compressive strength of the overlay concrete. In 1978, Tabor was the first to propose a slant shear test for the evaluation of the bond strength of prismatic specimens [37]. The composition of the concrete used for the repair material affects the interface concrete strength. Julio et al. mentioned that the added concrete and the concrete substrate having the same compressive strength cause an increase in the bond strength [38]. Saldanha et al. observed higher interface shear strength values for high- density specimens compared to the specimens with light weight aggregate concrete [39]. Previous studies revealed that the interface bond strength depends upon the adhesion and friction along the concrete

interface [31, 33, 40]. Gomaa et al. studied the effects of interface angle on the frictional resistance and failure pattern considering alkali activated concrete as the repair material [33]. Austin et al. suggested that the interface angle of the bond plane influences the ultimate load and failure pattern of the test specimen [41]. A cohesive failure pattern was noticed for the specimens with the lowest interface angle [42] and with an increased surface roughness [38]. Julio et al. noticed the cohesive failure pattern of slant shear specimens with different compressive strength, but observed adhesive failure for the specimens having the same compressive strength [43]. Later on, Santos and Julio found that both differential shrinkage and differential stiffness influence the bond strength of the slant shear test specimens. [44]. The interface bond plane under compression loading has both the compression and shear stresses due to the sliding of the top and bottom prisms at the concrete-to-concrete joint [45, 46]. Thus, the stress state acting on the bond plane affects the bond strength significantly. The shear force and the difference in the shrinkage between the old substrate and the new repair material produced shear stresses at the interface [47]. Tensile and shear stresses are induced in the repair material due to restrained shrinkage [48, 49]. The shrinkage of repair material or overlay can cause cracks or debonding in the structure, reducing load-carrying capacity and interface bonding, ultimately leading to failure [50]. It is also reported that the incompatibility between the repair material and the concrete arising from the high shrinkage levels results in the failure of a repair material [51]. Studies conducted by Sun et. al revealed that among the various bond tests like direct tensile, slant shear and push-out tests, the highest bonding strength is for the slant shear test [35]. Due to the better reliability of the slant shear test results [46, 47, 52], it is considered as an appropriate method to determine the interface shear bond strength in concrete. Hence the slant shear test was chosen in the present study for measuring the interaction of GP concrete in the bond plane.

Though strength is the primary factor of concern for concrete structures, durability has a significant role in the serviceability of the structures. Hence the present study considered both strength evaluation and determination of durability parameters like sorptivity, chloride penetrability, drying shrinkage and moisture movement of the hybrid GP concrete. No standard test methods are available to determine the shear strength of concrete cubes. The present study attempts to evaluate the shear strength of concrete cubes consisting of substrates and a repair material with hybrid GP concrete since it is not available in any past research. From the literature, it is seen that the slant shear test is one of the possible methods to assess the interfacial bond characteristics in concrete. In the shear cube test, failure occurs along two shearing surfaces under a compressive load application, while in the slant shear test failure occurs along an inclined plane slanted at an angle of 30^0. A combined effect of shear and compression is encountered while conducting the shear tests.

Factors like the compressive strength of both the substrate concrete (old layer) and the overlay concrete (new layer), density of concrete and the inclination of the bond plane with the loading axis influence the bond characteristics. However, there is a lack of information in the literature regarding the bond effects of the GP concrete when used as an overlay concrete. Hence, the present study is intended to investigate the bonding between the concrete containing hybrid GP and the normal concrete (GP0) by conducting a slant shear test. Tests were conducted on specimens with three concrete mix grades cured for seven and twenty-eight days. Since the study focuses on the determination of interface shear bond behavior of GP concrete, the angle of the interface bond plane was kept at 30^0 with the

vertical plane for all the slant shear test specimens to enforce adhesive failure in the GP specimens.

A wider range of analyses were carried out in the experimental program for studying the effect of hybrid GP in the interface bond strength characteristics of concrete. The objectives include:

i) To assess the mechanical properties of M30, M40 and M50 grades of concrete mixes simultaneously incorporating hybrid GP, two grades of GP in equal proportions (GP1:GP2 = 0.5:0.5), as a partial cement substitute at 10 % increment by weight of cement for each mix, till the attainment of better cube compressive strength.

ii) To evaluate the durability characteristics like sorption, chloride permeability, drying shrinkage and moisture movement at the same cement replacement levels and in the same concrete mix grades as above.

iii) To determine the interface shear bond strength and slant shear failure mode of the concrete composite specimens with normal concrete (M30) as substrate and an overlay of hybrid GP concrete with cement replacement level providing better strength and durability characteristics.

1.1 Research significance

Due to urbanization, the usage of glass is increasing tremendously resulting in the generation of a huge amount of waste glass. On account of the high recycling cost associated with the production processes of the waste glass to produce new glass, it is better to reuse waste glass as a concrete ingredient which requires only crushing the decontaminated waste glass in a ball mill to the required size. Hence, a mass volume of waste glass could be consumed by its utilization in the concrete sector focusing on a circular economy. Several studies were done on GP concrete for the determination of mechanical and durability properties. However, investigation of concrete containing GP on the shear strength of concrete cubes, or the interface bond strength of GP concrete for its application in repair or strengthening works or as an overlay for pavement construction has not been carried out. In the present study, strength of composite GP concrete cubes in shear with normal concrete as substrate (M30) and hybrid GP concrete of different mix grades (M30, M40 and M50) as repair material are evaluated. Hybrid GP, which was obtained by the combination of two particle sizes of GP in equal proportions (GP1:GP2 = 0.5:0.5), was used to improve the filling effect of the microstructure. To compare the shear performance, specimens were also cast with M30 grade concrete as substrate and different mix grades as overlay concrete (M30GP0, M40GP0, M50GP0). The behavior of GP concrete as an overlay concrete is not well-established, and the concrete structures usually encounter a combination of shear and compressive stresses; hence, the present study attempts to evaluate the bonding strength between concrete-to-concrete interface containing hybrid GP by conducting a slant shear test. In brief, the present investigation aims at studying the effect of utilizing hybrid GP concrete for repair purposes and as an overlay material by assessing the interfacial shear bond strength and slant shear failure mode of concrete comprising normal concrete of M30 grade as substrate, and normal as well as hybrid GP concretes having different compressive strengths as an overlay. Furthermore, the repair or overlay material should exhibit adequate strength and durability apart from its interface bond strength for ensuring the serviceability of repaired concrete constructions. Hence it is imperative to verify the strength and durability characteristics in addition to the interface bond strength of the hybrid GP concrete.

2. Materials and Methods

2.1 Microanalysis of cementing materials

Cementing materials used consisted of 53-grade ordinary Portland cement

(designated as PC) according to ASTM C150: 2015 [53] and commercially available GP with different fineness (designated as GP1 and GP2). The two grades of GP were included in the mix design to produce a well-graded mix with increased packing density. Manufactured sand (M-sand) of specific gravity 2.65 was used as fine aggregate due to its increased usage in the production of concrete than river sand. The fine aggregate conformed to zone II according to IS 383: 2016 [54]. The coarse aggregate complying IS standards [55] had a maximum size of 20 mm and a specific gravity of 2.7. CERA Hyperplast XR-W40 having a specific gravity of 1.2 was used as the superplasticiser.

Physical properties of the cementing materials comply with the ASTM specifications [53] and are tabulated in Table **1**. Scanning electron microscopy (SEM) , X-ray diffraction (XRD), carbon-hydrogen-nitrogen (CHN) analysis, energy-dispersive X-ray spectroscopy (EDS), particle size analysis (PSA), loss on ignition (LOI) and thermogravimetric analysis (TGA) were performed to find the microstructural features like the morphological characteristics, amorphous nature, fine particle size, reduced surface area, non-evaporable water content, mass loss and thermal behavior of the cementitious materials used in the experimental analyses.

Table 1. Physical properties and elemental composition of cement and glass powders.

Properties	PC	GP1	GP2
Specific gravity	3.15	2.73	2.7
Specific surface area (m^2/kg)	419.85	356.6	1360.6
Mean particle size (µm)	27.55	31.57	7.8
Loss on ignition (%)	2.8	1.8	1
SiO_2 (%)	21.9	77.2	72.6
CaO (%)	64.5	7.65	9.98
Fe_2O_3 (%)	3.66	0	-
Na_2O (%)	0.3	9.39	13.57
Al_2O_3 (%)	3.67	1.2	1.02
MgO (%)	0.78	2.21	3.83
K_2O (%)	1.47	0	-
SO_3 (%)	4.06	0	-

Fig. 1 provides the results of the analyses. SEM images (Fig. **1** 1a) reveal that GP2 specimen is compact due to its larger surface area and smaller particle size relative to GP1 and PC. Both GP particles exhibit smooth surfaces, while the cement particles exhibit size variations and irregular shapes. The XRD spectra (Fig. **1** 1b) of GP1 and GP2 show broad peaks, indicating their amorphous nature, whereas the narrow peaks of PC indicate its crystalline nature. Particle size distribution in Fig. **1**1c displays well-graded curves for PC, GP1 and GP2, representing a uniform distribution of particles for all cementing materials. Thermogravimetric analysis (TGA) shown in Fig. **1**1d reveals the decomposition of the cementing samples up to 800 ^{0}C temperature exposure. The results indicate that the GP particles exhibit higher resistance to high-temperature exposure compared to PC. CHN analysis (Fig. **1**1e) demonstrates lower levels of carbon, hydrogen and nitrogen in GP1 and GP2 compared to PC. This low CHN content in GP1 and GP2 contributes to decreased GHG emissions and promotes environmental sustainability.

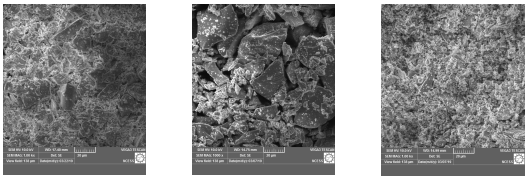

a) SEM images of PC, GP1, GP2

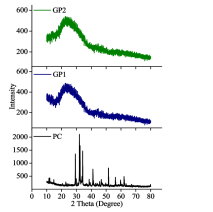

b) XRD images

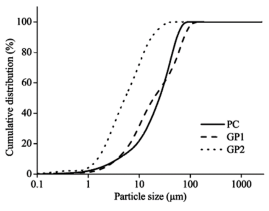

c)Particle size distribution

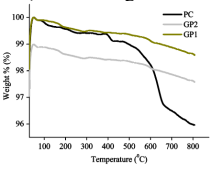

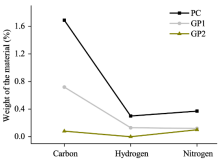

d)TGA graph e) CHN analysis

Fig. 1. Microstructural features of cementing materials.

It can be seen that the results of the microstructural analysis of both the GP particles are better or comparable to that of the ordinary Portland cement. The elemental composition of the cementing materials from EDS analysis is displayed in

Table **1**1. It is obvious from the sample analysis that the two grades of GP samples used in the current experimental investigation are micron-sized, amorphous, silica-rich sustainable materials and hence an appropriate partial substitute for cement.

2.2 Mix proportioning of concrete composite

Concrete mixes of M30, M40 and M50 grades were designed according to IS 10262 [56]. Details of the mix proportions with different percentage levels of GP are tabulated in

Table **2**. The concrete composite mixes with 0 %, 10 %, 20 %, 30 %, and 40 % by weight of GP are designated as GP0, GP10, GP20, GP30, and GP40, respectively.

Table 2. Details of concrete mix proportions (for 1 m^3).

Designation	Cement (kg)	Glass Powder (kg)		Fine aggregate (kg)	Coarse aggregate (kg)	Superplasticizer (kg)	w/b ratio
		GP1	GP2				
M30 GP0	319.4	0	0	697.3	1171.5	1.6	0.48
M30 GP10	287.46	15.97	15.97	697.3	1171.5	1.6	0.48
M30 GP20	255.52	31.94	31.94	697.3	1171.5	1.6	0.48
M30 GP30	223.58	47.91	47.91	697.3	1171.5	1.6	0.48
M30 GP40	191.64	63.88	63.88	697.3	1171.5	1.6	0.48
M40 GP0	368.8	0	0	651.2	1163.4	1.84	0.4
M40 GP10	331.92	18.44	18.44	651.2	1163.4	1.84	0.4
M40 GP20	295.04	36.88	36.88	651.2	1163.4	1.84	0.4
M40 GP30	258.16	55.32	55.32	651.2	1163.4	1.84	0.4
M40 GP40	221.28	73.76	73.76	651.2	1163.4	1.84	0.4
M50 GP0	388.2	0	0	641	1157.4	1.94	0.38
M50 GP10	349.38	19.41	19.41	641	1157.4	1.94	0.38
M50 GP20	310.56	38.82	38.82	641	1157.4	1.94	0.38
M50 GP30	271.74	58.23	58.23	641	1157.4	1.94	0.38
M50 GP40	232.92	77.64	77.64	641	1157.4	1.94	0.38

To obtain a well-graded mix with high packing density, the mean particle size of GP1 and GP2 obtained from PSA (size 31.57 and 7.80 μm, respectively), within the range of particle size of cement particles (27.60 μm) was used. Combination of the different grades of cementing particles used in the study resulted in a compact concrete mix with reduced voids, as smaller-sized particles fill the space between larger-sized particles.

2.3 Workability of concrete

Workability of the fresh concrete mix was measured by conducting a slump cone test based on ASTM C143-3:2003 [57].

2.4 Evaluation of mechanical properties

The cube compressive strength, flexural strength and split tensile strength were obtained from tests according to IS 516:2018 [58] using cube (150 mm sides) and prism (100 × 100 × 500 mm) specimens. Cylindrical (150 × 300 mm) specimens were used for obtaining the indirect tensile strength [58].

2.5 Evaluation of density of concrete

Mass of the oven-dried concrete cubes at 28-days age was recorded for the evaluation of density of GP concrete specimens. Density was calculated by

taking the ratio of mass to volume in compliance with ASTM C642:2013 [59].

2.6 Evaluation of durability characteristics

2.6.1 Sorptivity

Three identical specimens were prepared corresponding to each proportion of the mix (Fig. 2(a)). The curved surface of the pre-conditioned specimens was sealed as in Fig. 2(b) to enable one-dimensional sorption during immersion in water and the initial mass of the samples was taken. A schematic diagram of the test setup for conducting the sorptivity test following ASTM 1585-04:2007 [60] is shown in Fig. 2(c). The specimens were supported on rods to allow uniform exposure to water across the exposed surface with the intention of maintaining the water level at a depth of 5 mm as shown in Fig. 2(c). The gain in mass was observed initially at regular intervals of 1, 5, 10, 20, 30, and 60 minutes, then at an interval of 1 hour up to 6 hours, and later, at an interval of 1 day for up to 8 days. Finally, the water absorption and sorptivity were calculated using equations Eqs. (2.1)-(2.2) respectively.

$$I = \frac{\Delta m}{a \times d}, \tag{2.1}$$

where I is water absorption of the tested specimen in mm, Δm is increase in mass of the tested specimen in grams, a is contact area in mm^2 and d is density of water - $0.001 g/mm^3$.

$$S = \frac{I}{\sqrt{t}}, \tag{2.2}$$

where S is Sorptivity coefficient in $mm/s^{0.5}$.

a) Surface sealed specimens

b) Specimens on rods

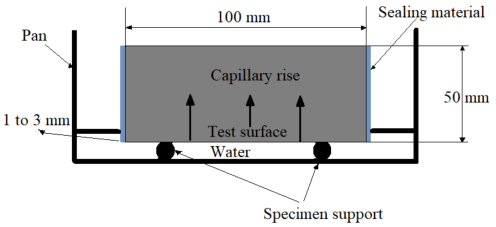

c) Sorptivity test setup ASTM 1585-04:2007

d) Vacuum saturation

e) RCPT test setup

Fig. 2. Durability test setup and conditioned test specimens.

2.6.2 Rapid Chloride Penetration Test (RCPT)

Cylindrical specimens with 100 mm diameter and 200 mm depth were cut into 50 mm thick slices as illustrated in Fig. 2(a) and the surface was coated with epoxy to prevent the loss of moisture. The specimens were subsequently set to vacuum saturation with de-aired water as shown in Fig. 2(d). Then the specimens were placed in the RCPT setup, where one face of the sample was in contact with a 0.3 N NaOH solution and the other face was in contact with a solution containing 3% NaCl as shown in Fig. 2(e) and tested according to ASTM C1202:2012 [61]. A potential difference of 60 V was maintained between the cathode (NaCl) and anode (NaOH) solutions, and the flow of electric charge was noted for 6 hours at an interval of 30 minutes. The total charge transmitted through the specimen was obtained using expression Eq. (2.3):

$$Q = 900\left(I_0 + I_{360} + 2\left(I_{30} + I_{60} + I_{90} + \cdots + I_{330}\right)\right), \tag{2.3}$$

where Q is charge passed and I_i is current passed in i minutes.

2.6.3 Drying shrinkage and moisture movement tests

For conducting the drying shrinkage test, ten concrete blocks (500 × 150 × 200 mm) of M30, M40 and M50 concrete mix with hybrid GP varying up to 40 % were cast and water-cured for 28 days. Three prisms of size 75 × 75 × 150 mm were cut from each concrete block and steel balls of 5 mm diameter were cemented at the centre of both ends of each specimen in accordance with IS 2185-1:2005 [62]. The specimens were then immersed in water for four days and were taken out and the initial length of each wet prism sample was measured using the length comparator to an accuracy of 0.0025 mm as shown in Fig. 3 (a). Then, the specimens were kept in a drying oven for 44 hours (Fig. 3 (b)). The length of the specimens was measured after cooling for four hours in a desiccator and the difference between the wet and dry length as a percentage of dry length was calculated. Similarly, the moisture movement test was conducted on the same specimens after being immersed in water for 4 days, complying with IS 2185-1:2005 [62].

a) Test setup b) Specimens in drying oven

Fig. 3. Drying shrinkage test.

2.7 Evaluation of bond by shear test

Shear tests were performed on 150 mm size shear cube specimens having 25 mm projections at the centre of one face and a cavity of 25 mm deep at the centre on the opposite face, both throughout the width of the specimen as shown in Fig. 4(a).

The casting of the shear cubes was done in two steps. Initially, two substrates of size 50 × 150 × 150 mm were cast at the two end portions of the cube moulds. After 14 days of curing, repair material was cast at the intermediate portion which is one-third width of the specimen. The two substrates were made of conventional concrete and the repair material with GP concrete of the same grade with better compressive strength. Three substrate-overlay combinations of the shear cubes were prepared, cured for 28 days and designated as M30 GP0- M30 GP30, M40 GP0 - M40 GP30 and M50 GP0 - M50 GP30. Shear under direct compression was applied and the load at which shearing takes place at the two interfaces was observed. Companion conventional concrete shear specimens of corresponding grades (M30 GP0, M40 GP0, M50 GP0) as well as GP shear cubes (M30 GP30, M40 GP30, M50 GP30) were monolithically cast, cured and tested for comparison. A photograph of the typical test specimens is shown in Fig. 4(b).

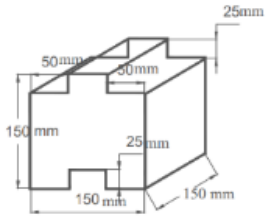

a) Specimen dimension

b) Photograph of test specimens

Fig. 4. Shear cube specimens.

Shear strength of cubes is calculated using Eq. (2.4).

$$Shear\ strength = \frac{Load}{A_s}, \qquad (2.4)$$

where A_s = Area of shear surfaces
= (150 – 25 - 25) × 150 × 2
= 30000 mm^2.

2.8 Evaluation of interface bond by slant shear test

The slant shear test under compression in accordance with British standards [63] and ACI concrete repair guide [64] was conducted on the specimens considering two curing regimes. Rectangular prismatic specimens of cross-section 100 × 100 mm, height of 400 mm and having an interface angle of 30^0 with the direction of applied force were cast.

a) Initial substrate b) Completed specimen

Fig. 5. Photograph showing the preparation of slant shear specimens.

Effects of three different grades of concrete (M30, M40, M50 grades) under 7 days and 28 days of curing as an overlay for the repair process, with and without GP, were investigated. In the case of all the slant shear test samples, the substrate was normal M30 grade concrete with a compressive strength of 39.04 N/mm^2. The surface of the substrates was prepared slightly rough and hand-brushed without exposing the aggregates so as to attain adequate bonding with the repair concrete layer or overlay. The overlay concrete selected for each test sample was normal as well as hybrid GP concrete with varying concrete grades such as M30, M40 and M50. The hybrid GP concrete with the highest compressive strength was used as the overlay. Accordingly, there are six substrate – overlay combinations in the investigation which are designated as M30 GP0 - M30 GP0, M30 GP0 - M30 GP30, M30 GP0 - M40 GP0, M30 GP0 - M40 GP30, M30 GP0 - M50 GP0 and M30 GP0 - M50 GP30. Four slant shear specimens were cast for each considered combination under two curing ages. The image showing the preparation of slant shear specimens is shown in Fig. 5.

Testing was conducted after 7 days and 28 days for the overlay concrete with a loading rate of 5 kN/s. Slant shear bond strength was determined using equation Eq. (2.5) and the interface normal strength was calculated using equation Eq. (2.6) [33, 41, 65].

$$f_s = \frac{F\cos\alpha\sin\alpha}{b^2}, \qquad (2.5)$$

$$\sigma = \frac{F\sin^2\alpha}{b^2}, \qquad (2.6)$$

where f_s is slant shear strength in N/mm^2, F is failure load in N, σ is average normal stress at the interface in N/mm^2, α is interface angle with the vertical axis = 30^0, b is width of the cross-section = 100 mm.

3. Results and Discussions

3.1 Workability of concrete

Workability of fresh concrete mix grades with varying cement replacements by slump cone procedure according to ASTM C143-3:2003 [57] is shown in Fig. 6.

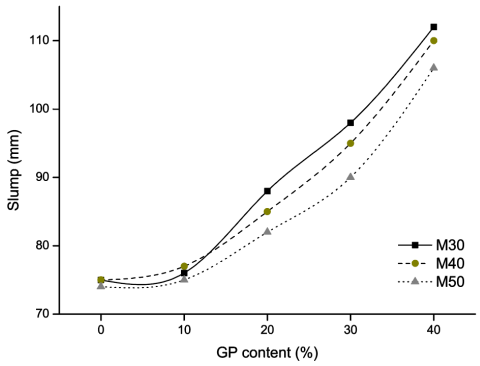

Fig. 6. Workability of concrete mixes.

Medium to high workability ranges were observed with the slump values between 70 to 110 mm, for the M30, M40 and M50 grade hybrid GP concrete mixes with GP percentage from 10% to 40%. The increase in

slump with an increase in the GP content was due to the smooth surface and low water absorption of GP. This low water demand of hybrid GP allows excess water availability in the concrete mixes. The slow hydration of hybrid GP in the concrete mix also enhanced the workability. The lower specific gravity of GP1 and GP2 than PC (refer Table **1**1) led to an increase in friction between the particles in the GP blended mixes due to its comparatively higher volume than GP0 mixes and hence the increased workability. The results confirm the previous findings [66, 67]. Thus, the addition of the two types of GP with different fineness enhances the workability of the concrete mix.

3.2 Concrete properties and mix proportion

Inclusion of hybrid GP as a cement substitute increased the hardened properties of the M30, M40 and M50 GP concrete mixes compared to the conventional mix at 30% cement replacement. The strength characteristics of the M30, M40 and M50 concrete grades with various percentages of hybrid GP content are tabulated in Table 3. The relationship of modulus of elasticity (E) of M30, M40 and M50 hybrid GP concrete grades with respective 28 days of compressive strength (f_{ck}) was calculated using the expression $E = 5000\sqrt{f_{ck}}$ and is shown in Table 3.

Table 3. Strength characteristics of hybrid GP concrete.

Grade of concrete	Hybrid GP content (GP1 + GP2) (%)	7 days compressive strength N/mm^2	28 days compressive strength N/mm^2	90 days compressive strength N/mm^2	28 days split tensile strength N/mm^2	28 days flexural strength N/mm^2	Elastic modulus N/mm^2
M30	0	26.07	39.04	40.81	3.54	4.32	31239.81
	10	25.41	38.37	41.70	3.82	4.88	30971.91
	20	27.26	40.59	44.22	3.96	4.96	31856.16
	30	**28.74**	**43.04**	**47.11**	**4.25**	**5.18**	32801.31
	40	25.63	38.81	42.07	3.11	3.68	31150.77
M40	0	31.56	50.22	52.59	4.1	4.8	35433.82
	10	30.07	48.59	52.67	4.25	4.8	34854.19
	20	31.11	49.93	54.44	4.53	5.2	35329.14
	30	**33.19**	**52.74**	**57.78**	**4.67**	**5.44**	36311.41
	40	29.48	48.15	52.07	4.03	4.64	34694.43
M50	0	38.81	59.85	61.93	4.6	5.2	38681.99
	10	37.19	58.37	62.52	4.95	5.44	38200.25
	20	39.85	60.15	64.59	5.24	5.6	38777.62
	30	**40.59**	**62.52**	**68.07**	**5.31**	**5.84**	39534.33
	40	36.15	58.07	61.19	4.39	4.8	38103.17

The study of hardened properties revealed that 30% replacement of cement with hybrid GP (GP30) produced better performance for all the mix grades in the study. Significant increase in the compressive strength of the hybrid GP concrete confirmed the pozzolanicity of the GP concrete due to the formation of calcium-silicate-hydrates. From the oxide composition of GP1 and GP2 (refer Table **1**1), both glass powders are considered as pozzolans according to physical and chemical requirements specified in ASTM C618:2014 [68]. The dense filling effect of the cementing particles also contributed an improvement in the compressive strength of GP concrete, which is substantiated by the well-graded particle size distribution curves of PC, GP1 and GP2 (Fig. **1**1c). Moreover, the improvement in compressive strength of hybrid GP concrete over normal concrete at 7 days and 28 days of age is observed at 30% cement replacement, while that at 90 days of age is observed at 10%, 20% and 30% cement

replacement levels for all concrete grades. This long-term strength gain is attributed to the delayed hydration process in hybrid GP concrete as confirmed by the previous studies [67, 69]. Furthermore, it is found that the compressive strength, split tensile strength, flexural strength, and modulus of elasticity increased with the increase in the percentage of replacement of cement up to 30% (GP30 mix) and thereafter decreased with a further increase in GP for all the grades of concrete. The decreased strength for a GP substitution of 40% was due to the inadequate quantity of calcium available in the mix for pozzolanic reaction. Hence, 30% GP substitution is regarded as the best level of cement replacement out of the considered grades of concrete under study.

3.3 Density of concrete

Variation of density for the oven-dried GP concrete cubes at 28 days is presented in Fig. 7. The decrease in the density of the GP concrete cubes with increase in the GP content (GP1:GP2 = 0.5:0.5) than the cubes of respective mixes without GP is observed. The reduced density of GP cubes is attributed to the low specific gravity of both GPs compared to Portland cement. It is clear from the results that the percentage variations in density between GP and normal concrete cubes are below 3% (up to 30% cement replacement) due to the increased packing effect of GP grains. The low variation in density of the GP concrete cubes is on account of the formation of the additional CSH crystals resulting in a dense microstructure with improved filling effect. The increased variation in density observed for GP40 for all the mix grades is due to reduced CSH crystal formation and consequent reduction in packing.

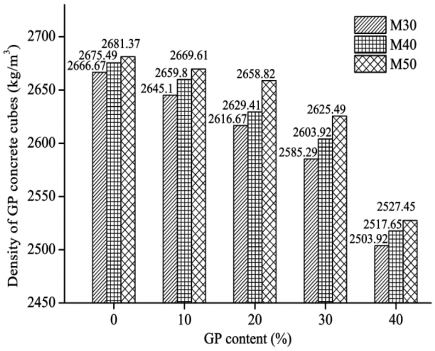

Fig. 7. Variation in density of GP concrete cubes.

3.4 Durability characteristics

3.4.1 Sorptivity

The penetration of water into the concrete pores by capillary suction was measured by placing the test specimens with only one surface exposed to water according to ASTM C1585-04:2007 [60].

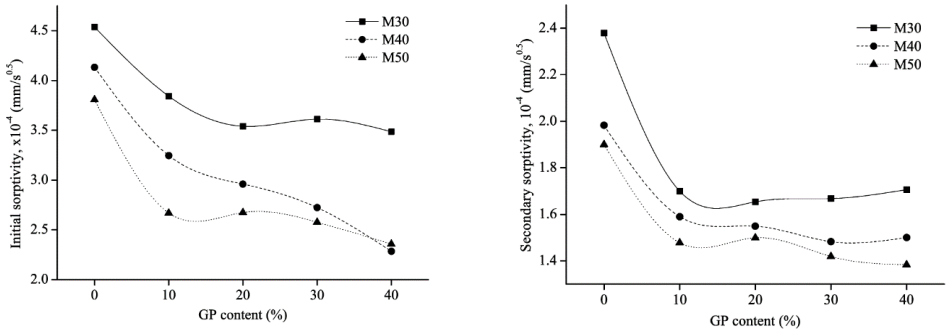

a) Initial sorptivity

b) Secondary sorptivity

Fig. 8. Sorptivity results.

Fig. 8(a)-(b) shows the effect of GP on the initial water sorptivity and secondary water sorptivity of concrete. The initial sorptivity and the secondary sorptivity

reduced substantially upon addition of the GP. Fig. 8 indicates a significant reduction in the sorptivity of M30, M40 and M50 grades with GP additions due to the improved surface layer characteristics of GP concrete. The reduction in the initial sorptivity is at a faster rate compared with secondary sorptivity. It is clear from the results that the use of GP effectively restricts the entry of water into the concrete. This reduction in sorptivity of GP concrete is a strong indication of its durability improvement.

3.4.2 Rapid Chloride Penetration Test (RCPT)

Results of the chloride-ion penetrability test, the charge passed (in Coulombs) versus GP content (%) plot for the test specimens of various concrete mix grades (M30, M40, M50) are rendered in Fig. 9.

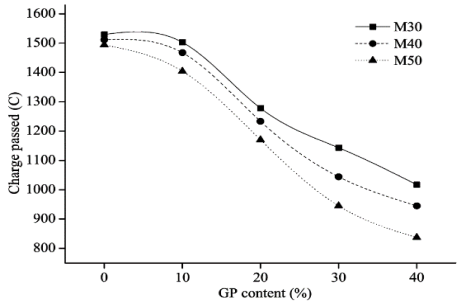

Fig. 9. RCPT results.

The total charge passed for six hours is graphically represented in Fig. 9. The maximum resistance to chloride-ion penetrability of the M30, M40 and M50 concrete mix grades is obtained for the specimens with 40 % replacement of cement by GP. The increased chloride-ion resistance is obtained from the filling effect of very fine GP particles in the concrete, which leads to a denser and less permeable microstructure. The refined microstructure of concrete is caused by the pozzolanic reactivity of GP in the concrete. It is inferred that since the chloride-ion penetrability is reduced to half for GP40 specimens, the GP concrete offers higher resistance to chloride-induced corrosion. The hydration of cement and GP renders increased resistance to chloride-ion penetration.

3.4.3 Drying shrinkage and moisture movement

The variations of shrinkage parameters with varying GP content of the M30, M40 and M50 mixes are shown in Fig. 10(a)-(b) respectively. The drying shrinkage values for all the mix grades increase with an increase in the GP content. The increase in GP percentage increases the presence of excess water due to the non-absorbent property of GP and this excess water was not used for the hydration of GP. The excess water surrounding the GP particles led to higher drying shrinkage deformation of the GP concrete compared to normal concrete. The expulsion of water held in the fine CSH gel of GP concrete results in a change in volume [48]. Since GP concrete is expected to have higher amounts of CSH gel, a higher amount of water is released which is the cause for increased drying shrinkage of GP specimens. Furthermore, M30 concrete grade experienced higher shrinkage compared to the higher concrete grades like M40 and M50. The high shrinkage values observed in M30 are attributed to the higher water content used for the M30 concrete mix preparation compared to that for M40 and M50 mix grades (refer

Table **2**). Hence, M30 concrete mix contains more water and exhibits higher drying shrinkage compared to M40 and M50 concrete grades for all cement replacements. However, it is observed that the drying shrinkage values are within the threshold limits of 0.06 % complying with Indian standards [62].

The percentage variation in shrinkage parameters of GP concrete is tabulated in Table 4. Moisture movement, which is a rewetting process, measures the reversible shrinkage of concrete. A decrease in the diffusion of water into the specimens with increased GP content as shown in Fig. 10(b) is due to the decreased pore spaces present in the GP concrete. The reduction in moisture

movement of the GP specimens compared to the normal concrete specimens is presented in Table 4. The impermeability of the mixes with an increase in the GP content is obvious from the results. The non-absorbent property of the GP also adds to the decreased moisture absorption. The moisture movement values obtained for all the test samples are within the permissible limit of 0.09 % based on Indian standards [62].

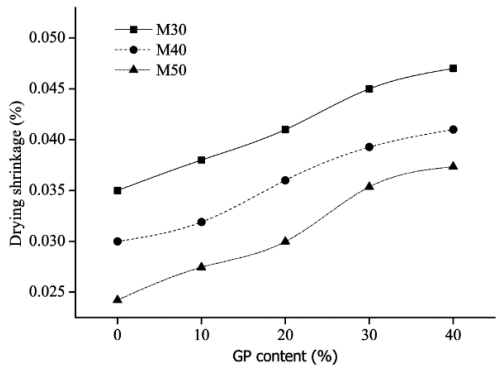

a) Drying shrinkage

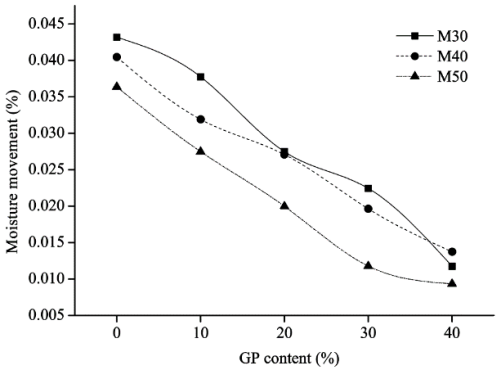

b) Moisture movement

Fig. 10. Variation in shrinkage parameters.

Table 4. Percentage variation in shrinkage parameters of GP concrete.

Specimen designation	Increase in drying shrinkage (%)			Reduction in moisture movement (%)		
	M30	M40	M50	M30	M40	M50
GP10	9.24	5.12	13.32	12.6	21.16	24.45
GP20	19.29	18.96	23.71	36.37	33.08	45.02
GP30	29.95	29.42	45.9	48.01	51.46	35.15
GP40	36.06	35.78	54.1	72.78	66.05	74.31

3.5 Shear cube test

Shear strength of the shear cube specimens under compression shows the failure of the two shearing surfaces as depicted in Fig. **11**. The failure of the shear specimens occurred along the known shear plane. Linear increase in the shear strength is observed for the M30, M40 and M50 grade GP concrete cubes in proportion to the compressive strength. The reduced water content in the corresponding higher grade concrete mixes also contribute to the increase in shear strength. The test specimens were subjected to shear stress along the bond plane with a slight bending stress. Monolithically cast shear cubes have continuous bonding since no interface plane exists in the cubes. The bond strength results of shear cubes demonstrated that the continuous bond cubes exhibited higher strength values than the repair shear cubes.

a) Shear failure of cubes with substrates and repair material

b) Shear failure of monolithically cast specimen

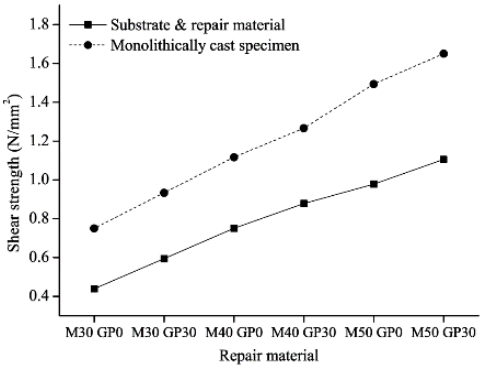

c) Shear strength of cubes

Fig. 11. Shear cube test results.

3.6 Slant shear test

Fig. 12 shows the slant shear compressive strength test results of overlay GP concrete with different compressive strengths, viz., M30, M40 and M50. In the investigation, the substrate for all the specimens is the M30 concrete grade without GP (normal concrete). Referring to the test results, it is observed that the compressive strength of the overlay concrete is an effective parameter that influences the slant shear bond strength. It is observed that the interface shear strength increases with an increase in the compressive strength of overlay GP concrete. The percentage increase in the slant shear strength for the M40 grade concrete at 28 days is 28.64% (for GP0) and 35.09% (for GP30) more than the substrate (M30 GP0), while that for M50 grade an increase of 53.30% (for GP0) and 60.14% (GP30) is observed. Parameters like compressive strength, drying shrinkage, elastic modulus, packing effect, hybrid GP content, etc. influence the slant shear strength. Increased bond strength observed for higher grades (M40 and M50) of hybrid GP concrete than M30 concrete grade is attributed to the decreased drying shrinkage for the higher grades of the GP concrete, as confirmed by the previous works [50, 51]. Higher elastic modulus observed for the higher GP concrete grades (M40 and M50) compared to M30 grade also influences the slant shear strength. There is no significant variation between the interface bond strengths for the mixes with higher overlay compressive strengths of M40 and M50, compared to the M30 concrete grade as shown in Fig. 12(d). This is due to the occurrence of partial failure of substrate concrete associated with an interface failure at high overlay compressive strengths of the GP concrete.

a) Pure adhesive failure

b) Adhesive failure with partial crushing

c) Adhesive failure surfaces

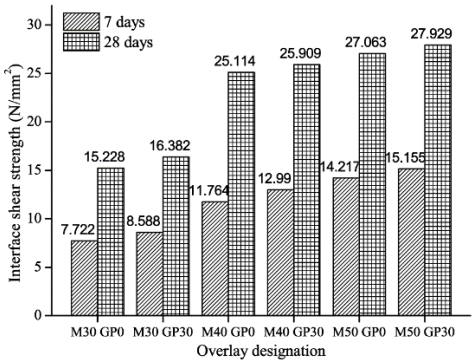

d) Interface shear strength

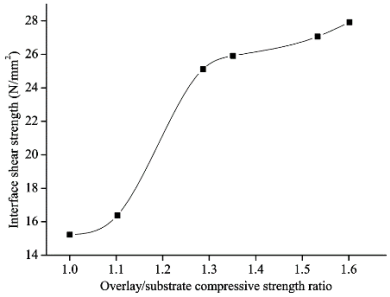

e) Interface shear strength vs overlay/substrate compressive strength ratio

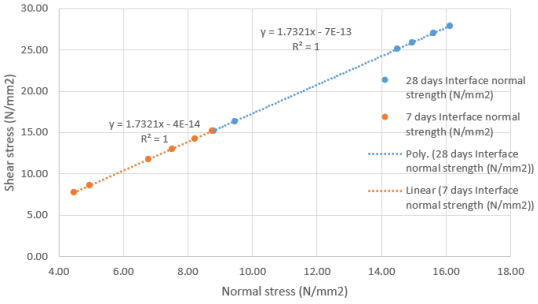

f) Shear stress vs normal stress at the interface

Fig. 12. Slant shear specimens.

From the results, it can be inferred that the usage of repair concrete (overlay concrete) with higher compressive strength than the substrate is advisable. In the present study it is observed that an increase of 35% in the compressive strength of overlay GP concrete gives better interface shear performance. The joint angle of the interface is inclined at 30˚ with the direction of the applied compressive force, hence, the interface is exposed to a combination of shear and compression and enforces adhesive failure. As both the substrate and overlay combinations of slant shear specimens of M30 grades, M30GP0 - M30GP0 and M30GP0 - M30GP30 possess the same range of strength, pure interface debonding (adhesive failure) occurred under loading in the test specimens as shown in Fig. 12 (a) and (c). The slant shear specimens with different

compressive strengths of substrate and overlay combinations, M30GP0 - M40GP0, M30GP0 - M40GP30, M30GP0 - M50GP0 and M30GP0-M50GP30, experienced interfacial failure along with partial substrate crushing as shown in Fig. 12(b), because the substrate has a lower strength than the overlay. There is no significant variation in the slant shear strengths for specimens with high strength overlay concrete which is due to the possibility of partial substrate crushing rather than the pure bond failure.

The ratio of overlay GP to substrate concrete compressive strength as a function of slant shear strength is shown in Fig. 12(e). It is obvious from the results that the slant shear strength has a significant effect up to the overlay GP/substrate concrete compressive strength ratio of 1.29, while for higher ratios only a marginal increase is observed. According to the equations, Eqs. (2.5)-(2.6), the correlation between the shear and normal stresses at the interface is shown in Fig. 12(f) [33, 41, 65].

4. Conclusion

The present study was carried out to assess the mechanical properties, durability characteristics and interface shear bond strength of the GP concrete incorporating two different fineness of GPs as partial cement substitute. Three grades of concrete mix were prepared for the experimental investigation. Based on the results, the following conclusions are drawn:

- The GP concrete possesses enhanced mechanical properties with the highest strength obtained for a cement replacement level of 30 % for all the concrete mix grades. Further addition of GP deteriorates the strength of concrete due to the inadequate amount of calcium present in the composite mix to form a secondary CSH structure.
- The percentage variation in density of the GP concrete is below 3 % for cement replacement levels up to 30 % due to the formation of additional CSH crystals, resulting in a dense microstructure with improved filling effect.
- The potential of GP as cement substitute is clearly established from the durability characteristics. The generation of CSH gel is obvious from the dense microstructure of GP concrete as observed from the chloride permeability and sorptivity studies. The longevity of GP concrete resulting from the low chloride penetration values indicate that GP concrete offers high resistance to corrosion.
- The shear cube strength of GP concrete as a repair material under compression is also improved with an increase in the grade of concrete.
- The enhanced performance of hybrid GP concrete in terms of mechanical, durability and interface shear bond strength ensure that the concrete incorporated with 30 % hybrid GP is suitable for retrofitting and strengthening works in addition to its application in new concrete works.

Thus, a viable waste management solution for discarded glass materials is aimed at by the utilisation of fine glass powders in hybrid form as a partial cement substitute.

Acknowledgement

The authors are grateful to the National Centre for Earth Science Studies (NCESS) and Central Laboratory for Instrumentation and Facilitation (CLIF) for performing the microstructural analysis. The work was supported by the Transportation Research Centre (TRC), Project ID: TRC20 CET RP2, College of Engineering Trivandrum, India and the All India Council for Technical Education (AICTE).

References

[1] Shayan A, Xu A. Performance of glass powder as a pozzolanic material in concrete: A field trial on concrete slabs. Cement and Concrete Research. 2006;36(3):457-68.

[2] Sobolev K, Türker P, Soboleva S, Iscioglu G. Utilization of waste glass in ECO-cement: Strength properties and microstructural observations. Waste Management. 2007;27(7):971-6.

[3] Schwarz N, Cam H, Neithalath N. Influence of a fine glass powder on the durability characteristics of concrete and its comparison to fly ash. Cement and Concrete Composites. 2008;30(6):486-96.

[4] Dhir RK, Dyer TD, Tang MC. Alkali-silica reaction in concrete containing glass. Materials and Structures/Materiaux et Constructions. 2009;42(10):1451-62.

[5] Khmiri A, Chaabouni M, Samet B. Chemical behaviour of ground waste glass when used as partial cement replacement in mortars. Construction and Building Materials. 2013;44:74-80.

[6] Siad H, Lachemi M, Sahmaran M, Hossain KMA. Effect of glass powder on sulfuric acid resistance of cementitious materials. Construction and Building Materials. 2015;113:163-73.

[7] Omran A, Tagnit-Hamou A. Performance of glass-powder concrete in field applications. Construction and Building Materials. 2016;109:84-95.

[8] Kalakada Z, Doh JH, Chowdhury S. Glass powder as replacement of cement for concrete–an investigative study. European Journal of Environmental and Civil Engineering. 2019;0(0):1-18.

[9] Patel D, Tiwari RP, Shrivastava R, Yadav RK. Effective utilization of waste glass powder as the substitution of cement in making paste and mortar. Construction and Building Materials. 2019;199:406-15.

[10] Elaqra HA, Al-Afghany MJ, Abo-Hasseira AB, Elmasry IH, Tabasi AM, Alwan MD. Effect of immersion time of glass powder on mechanical properties of concrete contained glass powder as cement replacement. Construction and Building Materials. 2019;206:674-82.

[11] Adesina A, Das S. Influence of glass powder on the durability properties of engineered cementitious composites. Construction and Building Materials. 2020;242:118199.

[12] Paul D, Bindhu KR, Matos AM, Delgado J. Eco-friendly concrete with waste glass powder: A sustainable and circular solution. Construction and Building Materials. 2022 Nov;355:129217.

[13] Elaqra HA, Alqahtani FK, Rustom R. Effect of curing temperature on mechanical behaviour of green concrete containing glass powder as cement replacement. Advances in Cement Research. 2021;33(10):458-68.

[14] Olofinnade OM, Ede AN, Ndambuki JM. Experimental investigation on the effect of elevated temperature on Compressive strength of concrete containing waste glass powder. International Journal of Engineering and Technology Innovation. 2017;7(4):280-91.

[15] Elaqra HA, Haloub MAA, Rustom RN. Effect of new mixing method of glass powder as cement replacement on mechanical behavior of concrete. Construction and Building Materials. 2019;203:75-82.

[16] Elaqra HA, Elmasry, Ibrahim H. Tabasi AM, Alwan, Mohammed D. Shamia HN, Elnashar MI. Effect of water-to-cement ratio and soaking time of waste glass powder on the behaviour of green concrete. Construction and Building Materials. 2021;299 (December 2020):124285.

[17] Xi J, Rui X, Yuetan M, Miaomiao Z, Yun B, Baoshan H. Influence of waste glass powder on the physico-mechanical properties and microstructures of fly ash-based geopolymer paste after exposure to high temperatures. Construction and Building Materials. 2019 Jul;201(April):369-79.

[18] Boukhelf F, Cherif R, Trabelsi A, Belarbi R, Bachir Bouiadjra M. On the hygrothermal behavior of concrete containing glass powder and silica fume. Journal of Cleaner Production [Internet]. 2021;318(April):128647.

[19] Soliman NA, Omran AF, Tagnit-Hamou A. Laboratory characterization and field application of novel ultra-high-performance glass concrete. ACI Materials Journal. 2016;113(3):307-16.

[20] Tariq S, Scott AN, Mackechnie JR, Shah V. Glass powder replacement in self-compacting concrete and its effect on rheological and mechanical properties. Journal of Sustainable Cement-Based Materials. 2021;0(0):1-17.

[21] Soliman NA, Tagnit-Hamou A. Partial substitution of silica fume with fine glass powder in UHPC: Filling the micro gap. Construction and Building Materials. 2017;139:374-83.

[22] Jain JA, Neithalath N. Chloride transport in fly ash and glass powder modified concretes - Influence of test methods on microstructure. Cement and Concrete Composites. 2010;32(2):148-56.

[23] Ramakrishnan K, Pugazhmani G, Sripragadeesh R, Muthu D, Venkatasubramanian C. Experimental study on the mechanical and durability properties of concrete with waste glass powder and ground granulated blast furnace slag as supplementary cementitious materials. Construction and Building Materials. 2017;156:739-49.

[24] Jain KL, Sancheti G GL. Durability performance of waste granite and glass powder added concrete. Constr Build Mater. 2020;252:1-11.

[25] Balasubramanian B, Gopala Krishna GVT, Saraswathy V, Srinivasan K. Experimental investigation on concrete partially replaced with waste glass powder and waste E-plastic. Construction and Building Materials. 2021;278:122400.

[26] Jiang X, Xiao R, Ma Y, Zhang M, Bai Y, Huang B. Influence of waste glass powder on the physico-mechanical properties and microstructures of fly ash-based geopolymer paste after exposure to high temperatures. Construction and Building Materials. 2020;262:120579.

[27] Cheng A, Chao SJ, Lin WT. Effects of leaching behavior of calcium ions on compression and durability of cement-based materials with mineral admixtures. Materials. 2013;6(5):1851-72.

[28] Marchand J, Bentz DP, Samson E, Maltais Y. Influence of Calcium Hydroxide Dissolution on the Transport Properties of Hydrated Cement Systems. Materials Science. 2001;113-29.

[29] "Shetty MS. Concrete Technology Theory and Practice. S. Chand & Company Ltd. Vol. 055. 2000. Available from: https://www.amieindia.in/downloads/ebooks/concrete-tech.pdf

[30] Liu S, Wang S, Zhou W, Li L, Xiao H, Wei J, et al. Strength and microstructure of mortar containing glass powder and/or glass aggregate. Journal Wuhan University of Technology, Materials Science Edition. 2016;31(6):1302-10.

[31] Costa H, Carmo RNF, Júlio E. Influence of lightweight aggregates concrete on the bond strength of concrete-to-concrete interfaces. Construction and Building Materials. 2018;180:519-30.

[32] Diab AM, Abd Elmoaty AEM, Tag Eldin MR. Slant shear bond strength between self compacting concrete and old concrete. Construction and Building Materials. 2017;130:73-82.

[33] Gomaa E, Gheni AA, Kashosi C, ElGawady MA. Bond strength of eco-friendly class C fly ash-based thermally cured alkali-activated concrete to portland cement concrete. Journal of Cleaner Production. 2019;235:404-16.

[34] Hassan A, Kawakami M, Matsuoka S, Tanaka H. Evaluation of bond strength between ultra-high performance reactive powder composite materials and fiber-reinforced concrete by slant shear test. American Concrete Institute, ACI Special Publication. 2004;SP-222(January 2004):215-29.

[35] Sun N, Song Y, Hou W, Zhang H, Wu D, Li Y, et al. Interfacial Bond Properties between Normal Strength Concrete and Epoxy Resin Concrete. Advances in Materials Science and Engineering. 2021;2021.

[36] Sahmaran M, Yücel HE, Yildirim G, Al-Emam M, Lachemi M. Investigation of the Bond between Concrete Substrate and ECC Overlays. Journal of Materials in Civil Engineering. 2014;26(1):167-74.

[37] Tabor LJ. The evaluation of resin systems for concrete repair. Magazine of Concrete Research. 1978;30(105):221-5.

[38] Júlio ENBS, Branco FAB, Silva VD. Concrete-to-concrete bond strength. Influence of the roughness of the substrate surface. Construction and Building Materials. 2004;18(9):675-81.

[39] Saldanha R, Santos P, Júlio E. Influence of concrete density and strength on the bond strength of composite members. fib Symposium TEL-AVIV 2013: Engineering a Concrete Future: Technology, Modeling and Construction, Proceedings. 2013;(April 2013):321-4.

[40] Clark LA, Gill BS. Shear strength of smooth unreinforced construction joints. Magazine of Concrete Research. 1985;37(131):95-100.

[41] Austin S, Robins P, Pan Y. Shear bond testing of concrete repairs. Materials and Structures,. 1999;29(28):249-59.

[42] Clímaco JCTS, Regan PE. Evaluation of bond strength between old and new concrete in structural repairs. Magazine of Concrete Research. 2001;53(6):377-90.

[43] Júlio ENBS, Branco FAB, Silva VD, Lourenço JF. Influence of added concrete compressive strength on adhesion to an existing concrete substrate. Building and Environment. 2006;41(12):1934-9.

[44] Santos PMD, Julio ENBS. Factors affecting bond between new and old concrete. ACI Materials Journal. 2011;108(4):449-56.

[45] Naderi M. Analysis of the slant shear test. Journal of Adhesion Science and Technology. 2009;23(2):229-45.

[46] Momayez A, Ehsani MR, Ramezanianpour AA, Rajaie H. Comparison of methods for evaluating bond strength between concrete substrate and repair materials. Cement and Concrete Research. 2005;35(4):748-57.

[47] Silfwerbrand J. Shear bond strength in repaired concrete structures. Materials and Structures/Materiaux et Constructions. 2003;36(260):419-24.

[48] Asad M, Baluch MH, Al-Gadhib AH. Drying shrinkage stresses in concrete patch repair systems. Magazine of Concrete Research. 1997;49(181):283-93.

[49] Mehta PK, Monteiro PJM. Concrete Microstructure, Properties, and Materials. 3rd ed. McGraw-Hill. McGraw-Hill; 2006. 1 to 684.

[50] Pattnaik RR. Investigation on Failures of Composite Beam and Substrate Concrete due to Drying Shrinkage Property of Repair Materials. Journal of The Institution of Engineers (India): Series A. 2017;98(1–2):85-93.

[51] Decter MH, Keeley C. Durable concrete repair - Importance of compatibility and low shrinkage. Construction and Building Materials. 1997;11(5-6):267-73.

[52] Saucier F, Bastien J, Pigeon M, Fafard M. A Combine Shear-comprehension Decive to Measure Concrete-to-concrete Bonding. 1981;

[53] ASTM C150:2015. Standard Specification for Portland Cement. Vol. i. 2015.

[54] IS 383:2016. Coarse and fine aggregate for concrete -specification. Vol. Third revi, Bureau of Indian Standards (BIS), New Delhi. 2016. p. 1-21.

[55] IS 2386 - Part III:2002. Method of Test for aggregate for concrete - Specific gravity, density, voids, absorption and bulking. Bureau of Indian Standards (BIS), New Delhi, India. 2002. p. 1-22.

[56] IS 10262:2019. Concrete Mix Proportioning-Guidelines (Second Revision), Bureau of Indian Standards (BIS) New Delhi. Bureau of Indian Standards (BIS) New Delhi. 2019. p. 1-27.

[57] ASTM C143M-03:2003. Standard Test Method for Slump of Hydraulic-Cement Concrete. Annual Book of ASTM Standards. 2003. p. 1–4.

[58] IS 516. Methods of Tests for Strength of Concrete. Vol. 59, Bureau of Indian Standards (BIS), New Delhi, India. 2018. p. 1-27.

[59] ASTM C642:2013. Standard Test Method for Density, Absorption, and Voids in Hardened Concrete, ASTM International, United States. Annual Book of ASTM Standards. 2013. p. 1-3.

[60] ASTM C1585-04:2007. Standard Test Method for Measurement of Rate of Absorption of Water by Hydraulic-Cement Concretes. American Society for Testing and Materials. 2007. p. 1-6.

[61] ASTM C1202:2012. Standard Test Method for Electrical Indication of Concrete's Ability to Resist Chloride Ion Penetration. American Society for Testing and Materials. 2012. p. 1-8.

[62] IS 2185-Part1:2005. Indian Standard Concrete masonry units, Part 1: Hollow and solid concrete blocks. Bureau of Indian Standards (BIS) New Delhi. 2005. p.17.

[63] EN 12615:1999. Products and systems for the protection and repair of concrete structures-Test methods-Determination of slant shear strength. BS; 1999.

[64] ACI 546R-04:2012. Concrete Repair Guide. Vol. 28, ACI. 2012. p. 0-15.

[65] Zanotti C, Borges PHR, Bhutta A, Banthia N. Bond strength between concrete substrate and metakaolin geopolymer repair mortar: Effect of curing regime and PVA fiber reinforcement. Cement and Concrete Composites. 2017;80:307-16.

[66] Aliabdo AA, Abd Elmoaty AEM, Aboshama AY. Utilization of waste glass powder in the production of cement and concrete. Construction and Building Materials. 2016;124:866-77.

[67] Soliman NA, Tagnit-Hamou A. Development of ultra-high-performance concrete using glass powder – Towards ecofriendly concrete. Construction and Building Material. 2016;125:600-12.

[68] ASTM C618:2014. Standard Specification for Coal Fly Ash and Raw or Calcined Natural Pozzolan for Use in Concrete, ASTM International, West Conshohocken, PA, 2012, www.astm.org. ASTM International. 2014. p. 1-5.

[69] Du H, Tan KH. Waste glass powder as cement replacement in concrete. Journal of Advanced Concrete Technology. 2014;12(11):468-77.